

RESEARCH ARTICLE | FEBRUARY 24 2017

# The use of a combined parametrised model for analysis of elastic scattering processes of $^{28}\text{Si}$ by different targets of $^{232}\text{Th}$ , $^{209}\text{Bi}$ and $^{197}\text{Au}$ at laboratory energy of 179MeV **FREE**

R. I. Badran



AIP Conf. Proc. 1809, 020008 (2017)

<https://doi.org/10.1063/1.4975423>



Boost Your Optics and Photonics Measurements

Lock-in Amplifier

Zurich Instruments

Find out more

Boxcar Averager

# The Use of a Combined Parametrised Model for Analysis of Elastic Scattering Processes of $^{28}\text{Si}$ by Different Targets of $^{232}\text{Th}$ , $^{209}\text{Bi}$ and $^{197}\text{Au}$ at Laboratory Energy of 179MeV

R. I. Badran

*Physics Department, Faculty of Sciences, The Hashemite University, P.O. Box 150459, Zarqa, Jordan*

*Corresponding author: rbadran@hu.edu.jo*

**Abstract.** A model that combines the parameterized Frahn-Venter scattering matrix with Regge pole factor, is employed to analyze the angular distribution of the elastic scattering processes  $^{28}\text{Si} + ^{232}\text{Th}$  and  $^{28}\text{Si} + ^{209}\text{Bi}$  and  $^{28}\text{Si} + ^{197}\text{Au}$  at laboratory energy 179 MeV. The effect of change in the size of target nucleus on the diffractive features of angular distribution of elastic scattering processes at fixed laboratory energy is examined. The theoretical results of angular distribution are fairly compared to the experimental data for the three elastic scattering processes at both forward and backward angles. The values of Regge pole parameters which are responsible for improving the fittings at backward angles are extracted from combined model. The total reaction cross sections in addition to other useful geometrical parameters for colliding nuclei are also obtained from the adopted model.

**Keywords:** Elastic scattering; Diffraction model; Frahn-Venter model; Regge pole model.

**PACS:** 25.70.--z, 25.70.Bc.

## INTRODUCTION

The numerical analysis of angular distribution for heavy-ion elastic scattering processes based on the partial wave expansion model in the presence of strong absorption were widely used [1–12]. In such analysis the detailed form of scattering matrix (*S*-matrix) around the grazing angular momentum, for strongly absorbed nuclei, can be neatly related to elastic scattering experimental data. Here, the *S*-matrix which represents the accumulative effect of the scattering potential on the incident wave might be determined experimentally by a partial wave fitting to the measured angular distribution of elastic scattering. A major contribution in the form of an analytical treatment of the partial wave expansion of elastic scattering cross-section was provided by Frahn and Venter [13]. This treatment made use of the semi-classical aspects of heavy-ion elastic scattering which are associated with the large values of orbital angular momenta involved and the short De Broglie wavelengths of projectile-target relative motion. The sum in the partial wave expansion was thus written in the form of an integral over a continuous angular momentum variable; while the  $\ell$ -dependence of the *S*-matrix was expressed in the form of generalized continuous

function which has the strong absorptive profile characteristic of heavy-ion elastic scattering. Closed form analytical expressions were thus derived for the elastic scattering cross-section [13]. This formalism gave a lucid physical picture of the “anatomy” of heavy-ion elastic scattering. In particular, it explained the mechanism and criteria for the diffractive aspects of elastic scattering as well as the refractive effects of the Coulomb and nuclear fields. It was also shown that a generalized expression for the cross section of elastic scattering of heavy ions is derived in order to give a quantitative description of very heavy ion data and to provide a simple method for determining the grazing angular momenta, interaction radii, diffuseness, and total reaction cross section [14]. This method might be used as an alternative to optical model analyses because it is simple and gives equivalent information about the interaction of very heavy ions. It was found that, the parametrised S-matrix is a source of important information which is needed in the theoretical calculations of transfer reactions based on strong absorption model (SAM) [10, 11]. Since most of the scattering amplitudes of nuclear optical potentials exhibit prominent Regge poles, then it became possible to insert a form factor that represents Regge poles into the parameterized scattering matrix elements of scattering amplitudes, in an approach based on partial wave expansion. It was also found that the insertion of this Regge pole factor had led to improve the fittings to the experimental data of angular distribution at backward angles [4-6, 14, 15].

The analysis of angular distribution for  $^{28}\text{Si} + ^{232}\text{Th}$  and  $^{28}\text{Si} + ^{209}\text{Bi}$  and  $^{28}\text{Si} + ^{197}\text{Au}$  elastic scattering at laboratory energy 179 MeV [16], using both FVM and combined model (in which the sum of Frahn-Venter parametrized scattering matrix elements and the Regge pole factor represent new modified scattering matrix elements) will be carried out. At first, for this projectile laboratory energy, the ratio of partial cross sections to Rutherford ones of elastic scattering, for a forward range of centre of mass angles, are calculated when the size of target nucleus is varying. Accordingly, the behavior of FVM parameters will be presented when the target nucleus change. Secondly, our analyses will be extended to improve the fall off fit of the angular distribution of elastic scattering at backward angles. This will be conducted by introducing the Regge pole formalism via inserting the Regge pole factor in the scattering matrix elements, following Mermaz et al approach, using parametrised scattering matrix of FVM as a background [4-6, 14].

## THEORETICAL BACKGROUND

The scattering amplitude  $f(\theta)$  of heavy ion elastic scattering is the sum of the nuclear,  $f_N(\theta)$ , and Coulomb,  $f_c(\theta)$ , scattering amplitudes, namely

$$f(\theta) = f_c(\theta) + f_N(\theta) \quad (1)$$

The nuclear scattering amplitude is written in partial wave analysis as [4-9]:

$$f_N(\theta) = (2ik)^{-1} \sum_{\ell=0}^{\infty} (2\ell+1) e^{2i\sigma_\ell} [S_{\ell,N} - 1] P_\ell(\cos\theta) \quad (2)$$

Here,  $\sigma_\ell$ ,  $k$ , and  $P_\ell(\cos\theta)$  are Coulomb phase shifts, wave number, and Legendre polynomials, respectively. The nuclear scattering matrix element  $S_{\ell,N} = \eta_\ell e^{2i\delta_{\ell,N}}$  where  $\eta_\ell$  is called the reflection coefficient and  $\delta_{\ell,N}$  is the real part of the phase shifts due to elastic scattering. Furthermore, the concept of nuclear phase shifts  $\delta_{\ell,N}$  is introduced into the partial wave to account for the effect of nuclear potential in the nuclear scattering.

In Frahn-Venter model, the scattering matrix elements  $S_{\ell,N}$  (in equation 2) become a continuous function  $S(\lambda)$  of the angular momentum  $\lambda$  where the summation over  $\ell$  in the partial wave expansion can be replaced by integration over  $\lambda$ . In FVM, the smooth variation of  $\eta_\ell$  and  $\delta_{\ell,N}$ , are represented by a differentiable function of the continuous variable  $\lambda = \ell + 1/2$  (i.e.  $\eta(\lambda)$  and  $\delta(\lambda)$ ), and the summation over  $\ell$  in the partial wave expansion, in equation 2, can be replaced by an integration over  $\lambda$  when a large number of partial waves are involved. Moreover, the grazing angular momentum value of  $\lambda$  becomes  $\Lambda$  and  $S_N(\lambda)$  must replace  $S_{\ell,N}$  [12, 13].

The nuclear scattering function in FVM has the expression [4, 12]:

$$S_N(\lambda) = [1 + e^{-\frac{(\lambda-\Lambda)}{\Delta}}]^{-1} + i\mu \frac{\partial}{\partial \lambda} [1 + e^{-\frac{(\lambda-\Lambda)}{\Delta}}]^{-1} \quad (3)$$

Here, the grazing angular momentum  $\Lambda$  and diffusivity parameter in  $\lambda$ -space  $\Delta$  together with the parameter  $\mu$  which represents the refractive strength of the nuclear interaction, will be the adjustable parameters for FVM calculations. Furthermore, the only requirement in FVM is that the absorptive shape function  $D_N(\lambda) = dS_N(\lambda)/d\lambda$  can be expressed with a simple Fourier transform, namely [4, 12]:

$$F_N(\Delta t) = \int_{-\infty}^{+\infty} D_N(\lambda) e^{i(\lambda-\Lambda)t} d\lambda \quad (4)$$

where  $t = \theta - \theta_R$ .

A simple classification to all scattering processes of charged particles above the Coulomb barrier [4-8] may be needed by knowing both Coulomb parameter  $n$  and the parameter  $h$  (which is the ratio of the center of mass kinetic energy  $E_{c.m.}$  to the Coulomb barrier  $V_c$ ). These two parameters together with the total reaction cross section from the generalized Fresnel model (GFM) and the corresponding relation from Fresnel model (FM) (which have special importance), are all expressed in Refs [4-6, 13].

The modified scattering matrix was formed when Regge pole factor is added to the S-matrix of Frahn-Venter [4, 5, 12]. The modified S- matrix, which has its two constituents as the Frahn-Venter parametrised form ( $S_\lambda^{FV}$ ) as the background S-matrix and the Regge pole factor, is expressed by [4, 6]:

$$S(\lambda) = S_\lambda^{FV} + \frac{iD(\lambda)e^{\lambda\phi_\lambda}}{\lambda - \lambda_c - i\Gamma(\lambda)/2} \quad (5)$$

where, a phase factor of  $e^{i\phi_{\lambda_0}}$  was introduced for the Regge pole and the amplitude of this pole is given by

$$D(\lambda) = D_0 [1 - \text{Re} S_{\lambda}^{FV}] \quad (6)$$

and its width is

$$\Gamma(\lambda) = \Gamma_0 [1 - \text{Re} S_{\lambda}^{FV}] \quad (7)$$

Both quantities in square brackets of equations (6) and (7) represent damping functions which play important role in avoiding unwanted oscillations of the angular distribution caused by high orbital angular momentum [4, 6]. Here, the parameters  $D_0$ ,  $\Gamma_0$ ,  $\lambda_0$  and  $\phi_{\lambda_0}$  represent reduced amplitude, reduced width, position and phase of Regge pole, respectively [4, 14]. The latter four parameters of Regge pole plus the three parameters of FV (namely,  $\Lambda$ ,  $\Delta$  and  $\mu$ ) are employed to get the fittings of angular distribution for the set of elastic scatterings, in the combined model. The combined model is developed to reproduce the cross sections of elastic scattering at two ranges of centre of mass angles (*i.e* forward and backward angles). This is because the parameterized model of FV cannot successfully reproduce, by itself, the cross sections at backward angles, especially for the systems that contain oscillations in their angular distribution.

## RESULTS and DISCUSSION

The calculated angular distribution for  $^{28}\text{Si} + ^{232}\text{Th}$ ,  $^{28}\text{Si} + ^{209}\text{Bi}$  and  $^{28}\text{Si} + ^{197}\text{Au}$  elastic scattering processes at laboratory energy 179 MeV using FVM only, are compared to experimental data as shown in Figure 1 (left panel) [16]. However, the best quality of fitting for each process of elastic scattering is judged visually and using  $\chi^2$  indicator. The parameters extracted from FVM model are shown in Table 1. It can also be noted that the value of the quarter point angle  $\theta_{1/4}$  for every projectile is comparable to the values of  $\theta_R$ . Also, the value of the ratio  $d/R$ , listed in Table 1, is mildly changing with the change in the mass of target. Here, the diffusivity parameter increases when the size of target nucleus increases. This is because the diffusivity parameter represents the width of the transition region in  $\ell$ -space, which becomes wider as the target nucleus gets larger. The total cross section exhibits linear dependence with  $A^{1/3}$ , as shown in Figure 1 (right panel), when the target nucleus is changed from  $^{197}\text{Au}$ ,  $^{209}\text{Bi}$ , to  $^{232}\text{Th}$  at a fixed incident energy of 179 MeV. This behavior is in accordance with the recipe of SAM. The quality of the theoretical results are found to be sensitive to the choice of the adjustable fitting parameters ( $\Lambda$ ,  $\Delta$  and  $\mu$ ) in FVM. For instance, the increase in the values of  $\Lambda$  resulted in pushing the highest peak of the structure towards smaller angles. Moreover, the increase in the value of  $\Delta$  is consistent with the increase in the slope of the cross-section fall off. Fraunhofer oscillations have been washed out by the Coulomb field. Furthermore, the change in values of  $\mu/2\Delta$  may be attributed to different fall off of cross sections at larger angles and also to varying effect of nuclear strength for different target nuclei.

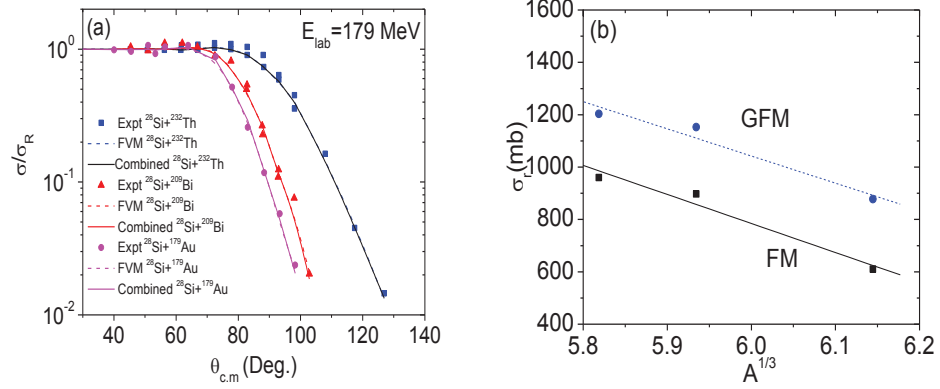


**Figure 1.** a) The experimental data (symbols) of angular distribution of elastic scattering of  $^{28}\text{Si} + ^{232}\text{Th}$ ,  $^{28}\text{Si} + ^{209}\text{Bi}$  and  $^{28}\text{Si} + ^{197}\text{Au}$  elastic scattering at laboratory energy 179 MeV are shown and compared to the theoretical results obtained using FVM model only (dashed line) and the combined model of Frahn-Venter and Regge (solid line); b) The total cross section versus  $A^{1/3}$  for different target nuclei ( $^{197}\text{Au}$ ,  $^{209}\text{Bi}$ , and  $^{232}\text{Th}$ ) at an incident energy of 179MeV using values of the total reaction cross sections extracted from both Simple Fresnel Model [FM] (square symbols) together with corresponding straight line fit (line) and Generalized Fresnel model [GFM] (circle symbols) together with corresponding straight line fit (dashed line).

**Table 1.** List of parameters for elastic scattering processes  $^{28}\text{Si} + ^{232}\text{Th}$ ,  $^{28}\text{Si} + ^{209}\text{Bi}$  and  $^{28}\text{Si} + ^{197}\text{Au}$  at laboratory energy 179 MeV, which are extracted from the analyses using both FVM only and Frahn-Venter plus Regge pole model (or combined model). The total reaction cross sections  $\sigma_r$  (FM) and  $\sigma_r$  (GFM) are obtained from Fresnel model (FM) and generalized Fresnel model (GFM), respectively.

Elastic scattering	$^{28}\text{Si} + ^{197}\text{Au}$	$^{28}\text{Si} + ^{209}\text{Bi}$	$^{28}\text{Si} + ^{232}\text{Th}$
$E_{\text{Lab.}}$ (MeV)	179	179	179
$\Lambda^*$	74	72	60
$\Lambda^{**}$	74	72	60
$\Delta^*$	8.856	9.48	11.085
$\Delta^{**}$	8.856	9.48	11.085
$\mu/2\Delta^*$	0.53	0.63	0.69
$\mu/2\Delta^{**}$	0.53	0.63	0.69
$r_o^*$ (fm)	1.42	1.425	1.4
$r_o^{**}$ (fm)	1.42	1.425	1.4
$d^*$ (fm)	0.48	0.49	0.49
$d^{**}$ (fm)	0.48	0.49	0.49
$\lambda_o^{**}$	30.12	35.11	39.11
$\phi_{\lambda_o}^{**}$ (Deg.)	45.9	48.2	50.2
$D_o^{**}$	10.3	10.8	11.8
$\Gamma_o^{**}$	7.4	7.9	8.2
$R^*$ (fm)	12.57	12.78	12.85
$R^{**}$ (fm)	12.57	12.78	12.85
$d/R^*$	0.0382	0.0383	0.0381
$d/R^{**}$	0.0382	0.0383	0.0381
$p^*$	73.8	71.99	57.89
$n^*$	68.9	72.388	78.49
$h^*$	1.24	1.21	1.13
$\theta_R^*$ (Rad)	1.5	1.576	1.83
$\theta_{1/4}$ (Rad) [Expt.]	1.46	1.54	1.78
$\theta_{\text{Nucl}}^*$ (Rad)	-0.03	-0.033	-0.031
$\sigma_r^{\dagger\dagger}$ (mb)	1203.6	1152.8	877.52
$\sigma_r^\dagger$ (mb)	960.03	897.5	610.08
$\chi^{2*}$	0.52	1.126	0.61
$\chi^{2**}$	0.0013	0.0029	0.0038

[Notes: \*, \*\*,  $\dagger\dagger$  and  $\dagger$  parameters extracted from FVM only, combined model, generalized Fresnel model (GFM) and simple Fresnel model (FM), respectively].

## CONCLUSION

The combined model exhibits marginal role in improving the quality of fittings in these elastic scattering processes as there is no apparent change in the Regge pole parameters. Moreover, the obtained parameters of FVM from combined model remain almost same as those obtained when FVM is used only. The results obtained from employing FVM are fairly compared to the experimental data. The behavior of the total cross section due to the change in the atomic mass of the target is as expected by strong absorption model.

## REFERENCES

1. J. A. McIntyre, K. H. Wang, L. C. Becker, *Phys. Rev.*, **117**, 1337-1338 (1960).
2. J. A. McIntyre, S. D. Baker, K. H. Wang, *Phys. Rev.*, **125**, 584-594 (1962).
3. M. C. Mermaz, *Zeitschrift für Physik A Hadrons and Nuclei*, **321**, 613-681 (1985).
4. R. I. Badran, I. H. Al-Lehyani, *Braz. J. Phys.*, **46**, 341-354 (2016).
5. R. I. Badran, A. I. Istiti, W. N. Mashaqbeh, I. H. Al-Lehyani, *Int. J. Mod. Phys. E*, 1550082 (2015).
6. R. I. Badran, H. Badahdah, *Braz. J. Phys.*, **39**, 684 (2009).
7. R. I. Badran, D. Al Masri, *Can. J. Phys.*, **91**, 355-364 (2013).
8. R. I. Badran, H. Badahdah, M. Arafah, R. Khalid, *Int. J. Mod. Phys. E*, **19**, 2199-2217 (2010).
9. R. I. Badran, *Act. Phys. Hung. A*, **21**, 151-160 (2003).
10. R. I. Badran, D. J. Parker, I. M. Naqib, *Euro. Phys. J. A*, **12**, 317-325 (2001).
11. R. I. Badran, M. I. Naqib, D. J. Parker, J. Asher, *J. Phys. G: Nucl. Part. Phys.*, **22**, 1441-1454 (1996).
12. W. E. Frahn, R. H. Venter, *Ann. Phys.*, **24**, 243-288 (1963).
13. W. E. Frahn, *Nuclear Physics A*, **302**, 267 – 280 (1978).
14. M. C. Mermaz, E. R. Chaves - Lomlei, J. Barrette, B. Berthier, A. Greiner, *Phys. Rev. C*, **29**, 147 (1983).
15. A. A. Cowley, G. Heymann, *Nucl. Phys. A*, **146**, 465 (1970).
16. A. Budzanowski, H. Dabrowski, L. Freindl, K. Grotowski, S. Micek, R. Planeta, A. Strazalkowski, M. Bosman, P. Leleux, P. Macq, J. P. Meulders, C. Pirart, *Phys. Rev. C*, **17**, 951 (1978).